THE JOURNAL OF BIOLOGICAL CHEMISTRY VOL. 284, NO. 6, pp. 3793–3803, February 6, 2009

Alzheimer Disease Aβ Production in the Absence of *S*-Palmitoylation-dependent Targeting of BACE1 to Lipid Rafts*[S]

Received for publication, November 25, 2008, and in revised form, December 12, 2008 Published, JBC Papers in Press, December 12, 2008, DOI 10.1074/jbc.M808920200

Kulandaivelu S. Vetrivel[‡1], Xavier Meckler[‡1], Ying Chen[‡], Phuong D. Nguyen[§], Nabil G. Seidah[¶], Robert Vassar[‖], Philip C. Wong[**], Masaki Fukata[‡‡], Maria Z. Kounnas[§], and Gopal Thinakaran[‡2]

From the [‡]Departments of Neurobiology, Neurology, and Pathology, The University of Chicago, Chicago, Illinois 60637, [§]TorreyPines Therapeutics, Inc., La Jolla, California 92037, the [¶]Laboratory of Biochemical Neuroendocrinology, Clinical Research Institute of Montreal, Montreal, Quebec H2W 1R7, Canada, the [‖]Department of Cell and Molecular Biology, The Feinberg School of Medicine, Northwestern University, Chicago, Illinois 60611, the [**]Department of Pathology, The Johns Hopkins University School of Medicine, Baltimore, Maryland 21205, and the [‡‡]Division of Membrane Physiology, National Institute for Physiological Sciences, National Institutes of Natural Sciences, Okazaki 444-8787, Japan

Alzheimer disease β-amyloid (Aβ) peptides are generated via sequential proteolysis of amyloid precursor protein (APP) by BACE1 and γ-secretase. A subset of BACE1 localizes to cholesterol-rich membrane microdomains, termed lipid rafts. BACE1 processing in raft microdomains of cultured cells and neurons was characterized in previous studies by disrupting the integrity of lipid rafts by cholesterol depletion. These studies found either inhibition or elevation of Aβ production depending on the extent of cholesterol depletion, generating controversy. The intricate interplay between cholesterol levels, APP trafficking, and BACE1 processing is not clearly understood because cholesterol depletion has pleiotropic effects on Golgi morphology, vesicular trafficking, and membrane bulk fluidity. In this study, we used an alternate strategy to explore the function of BACE1 in membrane microdomains without altering the cellular cholesterol level. We demonstrate that BACE1 undergoes *S*-palmitoylation at four Cys residues at the junction of transmembrane and cytosolic domains, and Ala substitution at these four residues is sufficient to displace BACE1 from lipid rafts. Analysis of wild type and mutant BACE1 expressed in BACE1 null fibroblasts and neuroblastoma cells revealed that *S*-palmitoylation neither contributes to protein stability nor subcellular localization of BACE1. Surprisingly, non-raft localization of palmitoylation-deficient BACE1 did not have discernible influence on BACE1 processing of APP or secretion of Aβ. These results indicate that post-translational *S*-palmitoylation of BACE1 is not required for APP processing, and that BACE1 can efficiently cleave APP in both raft and non-raft microdomains.

Alzheimer disease-associated β-amyloid (Aβ)[3] peptides are derived from the sequential proteolysis of β-amyloid precursor protein (APP) by β- and γ-secretases. The major β-secretase is an aspartyl protease, termed BACE1 (β-site APP-cleaving enzyme 1) (1–4). BACE1 cleaves APP within the extracellular domain of APP, generating the N terminus of Aβ. In addition, BACE1 also cleaves to a lesser extent within the Aβ domain between Tyr^{10} and Glu^{11} (β′-cleavage site). Processing of APP at these sites results in the shedding/secretion of the large ectodomain (sAPPβ) and generating membrane-tethered C-terminal fragments +1 and +11 (β-CTF) (5). The multimeric γ-secretase cleaves at multiple sites within the transmembrane domain of β-CTF, generating C-terminal heterogeneous Aβ peptides (ranging in length between 38 and 43 residues) that are secreted, as well as cytosolic APP intracellular domains (6). In addition to BACE1, APP can be cleaved by α-secretase within the Aβ domain between Lys^{16} and Leu^{17}, releasing sAPPα and generating α-CTF. γ-Secretase cleavage of α-CTF generates N-terminal truncated Aβ, termed p3.

Genetic ablation of *BACE1* completely abolishes Aβ production, establishing BACE1 as the major neuronal enzyme responsible for initiating amyloidogenic processing of APP (4, 7). Interestingly, both the expression and activity of BACE1 is specifically elevated in neurons adjacent to senile plaques in brains of individuals with Alzheimer disease (8). In the past few years additional substrates of BACE1 have been identified that include APP homologues APLP1 and APLP2 (9), P-selectin glycoprotein ligand-1 (10), β-galactoside α2,6-sialyltransferase

* This work was supported, in whole or in part, by National Institutes of Health Grants AG021495 and AG019070 (to G. T.). This work was also supported by Alzheimer's Association Grants IIRG (to G. T.) and NIRG (to K. S. V.), Canadian Institutes of Health Research Grant MOP 44363 (to N. G. S.), and an American Federation for Aging Research Fellowship (to X. M.). The costs of publication of this article were defrayed in part by the payment of page charges. This article must therefore be hereby marked "*advertisement*" in accordance with 18 U.S.C. Section 1734 solely to indicate this fact.

[S] The on-line version of this article (available at http://www.jbc.org) contains supplemental Figs. S1 and S2 and additional data.

[1] Both authors contributed equally to this study.

[2] To whom correspondence should be addressed: Knapp R212, 924 E. 57th St., Chicago, IL 60637. Tel.: 773-834-3752; Fax: 773-834-3808; E-mail: gopal@uchicago.edu.

[3] The abbreviations used are: Aβ, β-amyloid; APP, amyloid precursor protein; BACE1, β-site APP cleaving enzyme 1; CTF, C-terminal fragment; DHHC, Asp-His-His-Cys; DRM, detergent-resistant membrane; ELISA, enzyme-linked immunosorbent assay; FL, full-length; GPI, glycosylphosphatidylinositol; mAb, monoclonal antibody; MEF, mouse embryonic fibroblasts; PAT, protein acyltransferase; PLAP, placental alkaline phosphatase; PS, presenilin(s); WT, wild-type; IRES, internal ribosome entry site; TGN, trans-Golgi network; 3C/A, C478A/C482A/C485A; 4C/A, C474A/C478A/C482A/C485A.

(11), low-density lipoprotein receptor-related protein (12), β-subunits of voltage-gated sodium channels (13), and neuregulin-1 (14, 15), thus extending the physiological function of BACE1 beyond Alzheimer disease pathogenesis.

BACE1 is a type I transmembrane protein with a long extracellular domain harboring a catalytic domain and a short cytoplasmic tail. BACE1 is synthesized as a proenzyme, which undergoes post-translational modifications that include removal of a pro-domain by a furin-like protease, *N*-glycosylation, phosphorylation, *S*-palmitoylation, and acetylation, during the transit in the secretory pathway (16–20). In non-neuronal cells the majority of BACE1 localizes to late Golgi/TGN and endosomes at steady-state and a fraction of BACE1 also cycles between the cell surface and endosomes (21). The steady-state localization of BACE1 is consistent with the acidic pH optimum of BACE1 *in vitro*, and BACE1 cleavage of APP is observed in the Golgi apparatus, TGN, and endosomes (22–25). BACE1 endocytosis and recycling are mediated by the GGA family of adaptors binding to a dileucine motif (^{496}DISLL) in its cytoplasmic tail (21, 26–31). Phosphorylation at Ser^{498} within this motif modulates GGA-dependent retrograde transport of BACE1 from endosomes to TGN (21, 26–31).

Over the years, a functional relationship between cellular cholesterol level and Aβ production has been uncovered, raising the intriguing possibility that cholesterol levels may determine the balance between amyloidogenic and non-amyloidogenic processing of APP (32–34). Furthermore, several lines of evidence from *in vitro* and *in vivo* studies indicate that cholesterol- and sphingolipid-rich membrane microdomains, termed lipid rafts, might be the critical link between cholesterol levels and amyloidogenic processing of APP. Lipid rafts function in the trafficking of proteins in the secretory and endocytic pathways in epithelial cells and neurons, and participate in a number of important biological functions (35). BACE1 undergoes *S*-palmitoylation (19), a reversible post-translational modification responsible for targeting a variety of peripheral and integral membrane proteins to lipid rafts (36). Indeed, a significant fraction of BACE1 is localized in lipid raft microdomains in a cholesterol-dependent manner, and addition of glycosylphosphatidylinositol (GPI) anchor to target BACE1 exclusively to lipid rafts increases APP processing at the β-cleavage site (37, 38). Antibody-mediated co-patching of cell surface APP and BACE1 has provided further evidence for BACE1 processing of APP in raft microdomains (33, 39). Components of the γ-secretase complex also associate with detergent-resistant membrane (DRM) fractions enriched in raft markers such as caveolin, flotillin, PrP, and ganglioside GM1 (40). The above findings suggest a model whereby APP is sequentially processed by BACE1 and γ-secretase in lipid rafts.

Despite the accumulating evidence, cleavage of APP by BACE1 in non-raft membrane regions cannot be unambiguously ruled out because of the paucity of full-length APP (APP FL) and BACE1 in DRM isolated from adult brain and cultured cells (41). Moreover, it was recently reported that moderate reduction of cholesterol (<25%) displaces BACE1 from raft domains, and increases BACE1 processing by promoting the membrane proximity of BACE1 and APP in non-raft domains (34). Nevertheless, this study also found that BACE1 processing of APP is inhibited with further loss of cholesterol (>35%), consistent with earlier studies (32, 33). Nevertheless, given the pleiotropic effects of cholesterol depletion on membrane properties and vesicular trafficking of secretory and endocytic proteins (42–47), unequivocal conclusions regarding BACE1 processing of APP in lipid rafts cannot be reached based on cholesterol depletion studies.

In this study, we explored the function of BACE1 in lipid raft microdomains without manipulating cellular cholesterol levels. In addition to the previously reported *S*-palmitoylation sites (Cys^{478}/Cys^{482}/Cys^{485}) within the cytosolic tail of BACE1 (19), we have identified a fourth site (Cys^{474}) within the transmembrane domain of BACE1 that undergoes *S*-palmitoylation. A BACE1 mutant with Ala substitution of all four Cys residues (BACE1-4C/A) fails to associate with DRM in cultured cells, but is not otherwise different from wtBACE1 in terms of protein stability, maturation, or subcellular localization. Surprisingly, APP processing and Aβ generation were unaffected in cells stably expressing the BACE1-4C/A mutant. Finally, we observed an increase in the levels of APP CTFs in detergent-soluble fractions of BACE1-4C/A as compared with wtBACE1 cells. Thus, our data collectively indicate a non-obligatory role of *S*-palmitoylation and lipid raft localization of BACE1 in amyloidogenic processing of APP.

EXPERIMENTAL PROCEDURES

cDNA Constructs—Plasmids encoding C-terminal FLAG-tagged wtBACE1 and 3C/A (C478A/C482A/C485A) (19) and hemagglutinin-tagged Asp-His-His-Cys (DHHC)-rich protein acyltransferases (PATs) have been described (48). A plasmid containing placental alkaline phosphatase (PLAP) cDNA was obtained from ATCC (clone MGC-5096). BACE1-3C/A cDNA was used as the template to generate BACE1-4C/A (C474A/C478A/C482A/C485A) by PCR mutagenesis, and the amplified segment was verified by sequencing. BACE1-GPI cDNA was constructed by overlap PCR by replacing the transmembrane and C-terminal sequences of BACE1 with the GPI anchor domain from PLAP. For retroviral expression, the cDNAs were subcloned into retroviral vector, pMXpuro (provided by Dr. Toshio Kitamura, University of Tokyo, Japan) or pLHCX (Clonetech). To construct a retroviral vector for low-level transgene expression (pMXpuroIRES), we cloned the internal ribosome entry site (IRES) from pIRES (Clontech) downstream of the puromycin resistance cassette in pMX vector. BACE1 cDNAs were then subcloned downstream of the IRES.

Retroviral Infections and Generation of Stable Cell Lines—*BACE1*$^{-/-}$ mouse embryonic fibroblasts (MEF) have been previously described (49). N2a cells stably expressing c-Myc epitope-tagged wtAPP (N2a 695.13) and APP$_{Swe}$ (N2a Swe.10) have been described previously (24). The Plat-E retroviral packaging cell line was kindly provided by Dr. Toshio Kitamura (University of Tokyo, Japan). Retroviral infections were performed as described previously (50). Briefly, retroviral supernatants collected 48 h after transfection of Plat-E cells with expression vectors were used to infect *BACE1*$^{-/-}$ MEF or N2a cells in the presence of 10 μg/ml Polybrene. Stably transduced pools of MEF, N2a 695.13, or Swe.10 cells were selected in the presence of 4 μg/ml puromycin or hygromycin (400 μg/ml).

Antibodies—BACE1 was detected using rabbit polyclonal antibodies anti-BACE1 (residues 46–163 (4)) and 7523 (residues 46–60 (16)) (provided by Dr. Christian Haass, Ludwig-Maximilians-University, Munich), or monoclonal antibody (mAb) BACE1-Cat1 (residues 46–460 (8)) and anti-FLAG M2 (Sigma). Rabbit polyclonal antiserum CTM1 was raised against a synthetic peptide corresponding to the C-terminal 15 amino acids of APP followed by the c-Myc epitope (MEQKLISEEDLN). Rabbit polyclonal $PS1_{NT}$ antiserum (residues 1–65) has been described (51). Both mAb 26D6 (52) and B436 (53) (epitopes within residues 1–12 of Aβ) react with the NH_2-terminal region of Aβ and also recognize sAPPα; mAb B113 is selective for Aβ40 (53). The following mAbs were purchased from commercial sources: GM130, syntaxin 6, flotillin-2, γ-adaptin, EEA1 (BD Biosciences), anti-hemagglutinin (clone 16B12) and 4G8 (Covance), and mAb 5228 (Chemicon).

Lipid Raft Fractionation—Lipid rafts were isolated from 0.5% Lubrol WX (Lubrol 17A17; Serva) lysates of cultured cells by discontinuous flotation density gradients as described previously (40, 41). For the analysis of cell surface rafts, subconfluent cultures were surface biotinylated with NHS S-S biotin (Pierce) as described previously (24) and then subjected to lipid raft fractionation. Cell surface-biotinylated proteins in gradient fractions were captured with streptavidin beads (Pierce) and analyzed by immunoblotting. For quantifications, optimal exposures of Western blots were analyzed by standard densitometry, and a transmission calibration step tablet (Stouffer Industries, Inc.) was used to convert raw optical densities to relative fold-differences in signal intensity using Metamorph software (Molecular Devices).

Protein Analyses—Metabolic and pulse-chase labeling using [^{35}S]Met/Cys were performed essentially as described (24, 53). To assess the stability of BACE1, parallel dishes were pulse-labeled for 30 min with 250 μCi/ml [^{35}S]Met/Cys (MP Biomedicals) and chased for various time points. BACE1 was immunoprecipitated from cell lysates using anti-BACE1 antibody. For analysis of APP, cells were pulse-labeled for 15 min or continuously labeled for 3 h. Full-length APP and APP CTFs were immunoprecipitated from cell lysates using CTM1 antibody. Aβ and p3 fragments were immunoprecipitated from the conditioned medium using mAb 4G8. β-CTFs (starting at +1 residue of Aβ) were identified by probing the blots with mAb 26D6.

Aβ, sAPPα, and sAPPβ Measurements—Conditioned media were collected 48 h after plating the cells and the levels of secreted Aβ and sAPPα were quantified by ELISA as described previously (53). Aβ1–40, Aβx-40, and Aβ1-x were measured using specific sandwich ELISAs. Aβ peptides were captured using mAb B113 for Aβ1–40 and Aβx-40 ELISA, and mAb B436 for Aβ1-x ELISA. Bound peptides were detected using alkaline phosphatase-conjugated mAb B436 for Aβ1–40 ELISA or biotinylated mAb 4G8 in combination with the streptavidin-alkaline phosphatase complex for Aβx-40 and Aβ1-x ELISA. Alkaline phosphatase activity was measured using CSPD-Sapphire II Luminescence Substrate (Applied Biosystems) and relative luminescence unit values were measured using a standard 96-well luminometer. Each sample was assayed in duplicate using appropriate dilution of the conditioned media so that the relative luminescent units were in the linear range of the standards included on each plate. Synthetic Aβ40 peptide (Bachem) was diluted in culture medium to generate standard curve (ranging from 1 to 1000 pg/well). sAPPα was quantified by sandwich ELISA using mAb 5228 for capture and mAb B436 for detection, and quantified using a standard curve prepared using affinity-purified sAPPα as described (53). sAPPβ was quantified using a commercial sβAPP wild-type ELISA kit and Meso Scale Sector Imager 6000 (Meso Scale Discovery, Gaithersburg, MD) for detection following the manufacturer's recommended protocol. Captured sAPPβ was quantified by comparing the signals of the samples to a standard curve included on each plate prepared using recombinant sAPPβ in complete medium.

Analysis of BACE1 Palmitoylation—COS7 cells were cotransfected with BACE1 and DHHC plasmids using Lipofectamine 2000 (Invitrogen) and labeled 48 h after transfection. Stable pools of *BACE1*$^{-/-}$ MEF and N2a cells were grown to subconfluence prior to labeling. Cells were preincubated for 1 h in Dulbecco's modified Eagle's medium supplemented with 1 mg/ml fatty acid-free bovine serum albumin (Sigma) and labeled for 4 h with 0.5 mCi/ml [10,11-^{3}H]palmitic acid (American Radiolabeled Chemicals) diluted in the preincubation medium. Cells were scrapped in lysis buffer (150 mM NaCl, 50 mM Tris-HCl, pH 7.4, 0.5% Nonidet P-40, 0.5% sodium deoxycholate, 5 mM EDTA, 0.25% SDS, 0.25 mM phenylmethylsulfonyl fluoride, Roche Protease Inhibitor Mixture 1X), and sonicated for 30 s on ice. Aliquots of lysates (adjusted to trichloroacetic acid precipitable radioactivity) were incubated overnight with 2 μl of anti-FLAG M2 antibody to immunoprecipitate BACE1. Immunoprecipitates were fractionated by SDS-PAGE, transferred to polyvinylidene difluoride membrane (Bio-Rad), and [^{3}H]palmitic acid-labeled BACE1 was detected by PhosphorImager analysis (GE Healthcare). The membranes were subsequently subject to Western blotting with FLAG M2 antibody (1:20,000) to reveal total immunoprecipitated BACE1. To compare the relative efficiencies of BACE1 palmitoylation by each DHHC, the ratio between [^{3}H]palmitic acid-labeled BACE1 and immunoblot BACE1 signal intensities were quantified using Image J software.

Immunofluorescence Microscopy—Cells cultured on poly-L-lysine-coated coverslips were fixed using 4% paraformaldehyde. Polyclonal BACE1 antiserum 7523 and mAb against γ-adaptin or transferrin receptor were diluted in phosphate-buffered saline containing 3% bovine serum albumin and 0.2% Tween 20, and incubated with fixed cells at room temperature for 2 h. Images were acquired on a Zeiss confocal microscope (Pascal) using ×100 1.45 NA Plan-Apochromat oil objective. Images were processed using Metamorph software (Molecular Devices).

RESULTS

BACE1 Is S-Palmitoylated at 4 Cysteine Residues—Previously it was reported that BACE1 is *S*-palmitoylated at three Cys residues (Cys^{478}, Cys^{482}, and Cys^{485}) within its cytosolic tail (Fig. 1*A*) (19). In stably transduced *BACE1*$^{-/-}$ MEF, overexpressed wtBACE1 can be readily labeled with [^{3}H]palmitic acid (Fig. 1*B*). As described previously, labeling was significantly

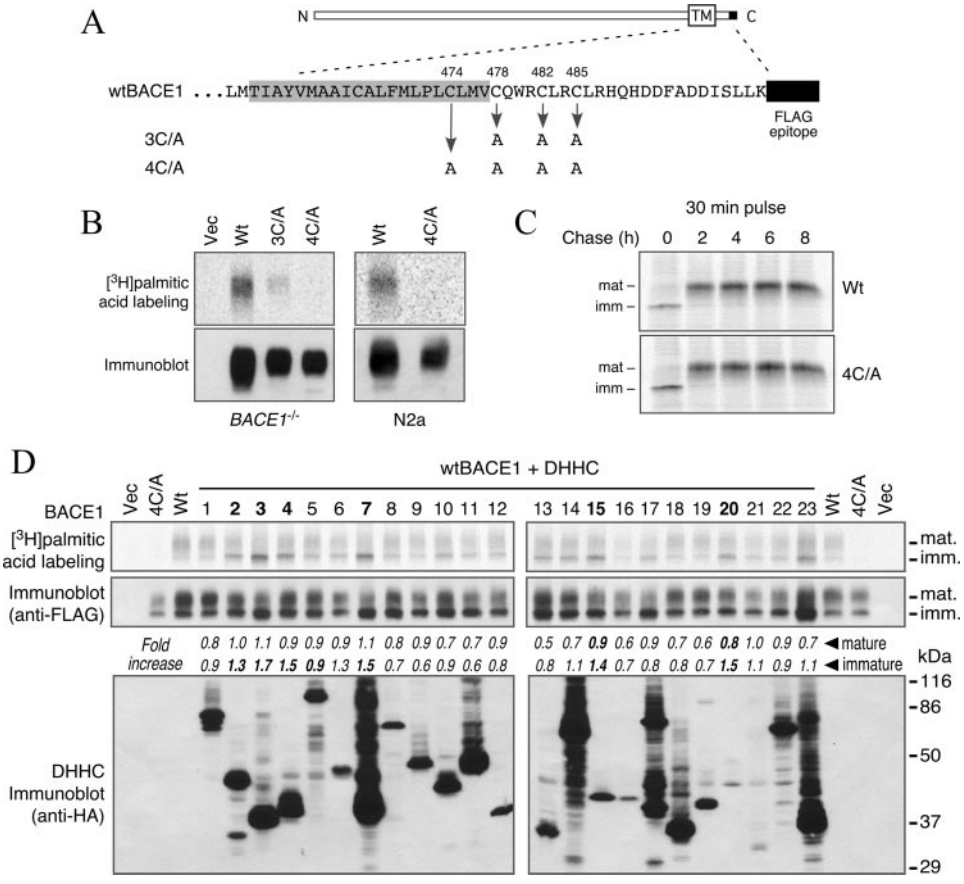

FIGURE 1. ***S*-Palmitoylation of BACE1.** *A*, the structure of BACE1. The predicted transmembrane domain is *shaded* and *S*-palmitoylated Cys residues are marked in wtBACE1. *3C/A* and *4C/A* represent BACE1 with 3 or 4 Ala substitutions. *B*, stable pools of *BACE1*$^{-/-}$ MEF or N2a cells harboring empty vector or indicated BACE1 cDNA were labeled with [^{3}H]palmitic acid for 4 h and cell lysates were analyzed by immunoprecipitation with FLAG mAb. After exposure to PhosphorImager screens, the membranes were immunoblotted with FLAG mAb. *C*, N2a cells stably expressing wtBACE1 and 4C/A cells were pulse-labeled with [^{35}S]Met/Cys for 30 min, and chased for the indicated period of time in the presence of cycloheximide. BACE1 was immunoprecipitated from lysates at each time point and analyzed by SDS-PAGE and phosphorimaging. *D*, COS7 cells were cotransfected with wtBACE1 and each of the DHHC PATs and labeled with [^{3}H]palmitic acid. BACE1 was then immunoprecipitated from cell lysates and analyzed by phosphorimaging (*top panel*) or immunoblotting (*middle panel*). The expression of DHHC PATs in the corresponding samples is shown in the *lower panel*. The normalized ratio of [^{3}H]palmitic acid to immunoblot signal is indicated as DHHC-induced fold-change in the efficiency of BACE1 palmitoylation. DHHC3, 4, 7, 15, and 20 significantly increased immature BACE1 palmitoylation.

reduced, but still clearly detectable, in MEF stably expressing a BACE1 mutant (BACE1-3C/A) harboring Cys to Ala substitutions at the three Cys residues previously identified as the sites of *S*-palmitoylation (Fig. 1*B*). This suggested that additional site(s) in BACE1 might be *S*-palmitoylated. To test whether Cys^{474} located within the putative transmembrane domain is a target site for *S*-palmitoylation, we introduced Cys to Ala substitutions at this position. Stable MEF pools expressing combined substitution of all the four Cys residues with Ala (BACE1-4C/A) completely abolished *S*-palmitoylation of BACE1 when stably expressed in *BACE1*$^{-/-}$ MEF (Fig. 1*B*). These results were confirmed by stably expressing the wtBACE1 and BACE1-4C/A mutant in neuronal (N2a) cells. These results indicate that BACE1 is palmitoylated at four Cys residues located in the cytoplasmic membrane boundary.

S-Palmitoylation Is Not Required for Stability of BACE1—Post-translational *S*-palmitoylation is known to function as a regulatory mechanism, which in many cases confers stability to the target protein (reviewed in Ref. 54). Examples include γ-secretase subunits nicastrin and APH-1, sortilin, cationic-independent mannose 6-phosphate receptor, chemokine receptor CCR5, human A1 adenosine receptor, and Rous sarcoma virus transmembrane protein (54–56). Therefore, we performed pulse-chase experiments using [^{35}S]Met/Cys labeling to test the stability of nascent wtBACE1 and palmitoylation-deficient BACE1 mutant. Parallel dishes of N2a cells stably expressing either wtBACE1 or BACE1-4C/A were pulse-labeled for 30 min and chased for varying lengths of time in the presence of cycloheximide. At the end of the chase period, the cell lysates were prepared and analyzed by immunoprecipitation with anti-BACE1 antibodies. In agreement with previous findings (16), maturation of wtBACE1 into a complex glycosylated protein with markedly reduced migration on SDS gels was evident at 2 h of chase. Mature wtBACE1 was relatively stable up to 8 h of chase (Fig. 1*C*). Maturation and stability of BACE1-4C/A were indistinguishable from that of wtBACE1. These results indicate that *S*-palmitoylation is not required for the stability of BACE1.

Characterization of BACE1 S-Palmitoylation by DHHC Family of Protein Acyltransferases—A family of 23 integral membrane PAT, which share a characteristic DHHC-cysteine-rich domain, mediate protein palmitoylation in human (48). Co-expression of individual PATs with the substrate protein to screen for PAT that increase incorporation of radiolabeled palmitate is the method of choice to identify a cognate enzyme-substrate pair. This pioneering approach was established first for the identification of PATs that specifically enhanced palmitoylation of neuronal scaffold protein PSD-95 (48). Using this approach, we sought to identify the PATs that increased palmitate incorporation into BACE1. We co-transfected COS7 cells individually with each of the 23 DHHC cDNAs and wtBACE1, and examined *S*-palmitoylation of BACE1 by [^{3}H]palmitic acid labeling and immunoprecipitation (Fig. 1*D*). In this experiment, we also used BACE1-4C/A as an internal negative control for the lack of [^{3}H]palmitic acid labeling of BACE1. Transfection of BACE1 in COS7 cells allowed us to detect both immature and mature (complex glycosylated) BACE1 (Fig. 1*D*). We found that several DHHC PATs increased [^{3}H]palmitate labeling of BACE1, especially the immature form. Quantification of [^{3}H]palmitate incorporation relative to signal intensity of immunoblots

revealed that co-expression of DHHC 3, 4, 7, 15, and 20 enhanced immature BACE1 palmitoylation by 1.4–1.7-fold (Fig. 1*D*). *S*-Palmitoylation of immature, core glycosylated BACE1 in transiently transfected COS7 cells indicates that nascent BACE1 can undergo *S*-palmitoylation in the endoplasmic reticulum or during early secretory trafficking through the Golgi apparatus.

S-Palmitoylation Does Not Affect the Subcellular Localization of BACE1—BACE1 undergoes complex post-translational modifications that are particularly important in defining its subcellular organelle destination and steady-state distribution. For example, reversible acetylation in the luminal domain of BACE1 regulates its stability as well as exit from the ER (20, 57). Moreover, phosphorylation regulates the fate of BACE1 endocytosed from the cell surface; whereas phosphorylated BACE1 is transported from the endosomes to the TGN, non-phosphorylated BACE1 is directly recycled to the cell surface (18, 29). Therefore we sought to investigate the importance of palmitoylation on subcellular localization of BACE1. To this end, we performed immunofluorescence microscopy analysis of wtBACE1 and BACE1-4C/A. The polyclonal antibody 7523 did not show any background staining in *BACE1*$^{-/-}$ MEF transduced with an empty retroviral vector. In agreement with previous reports (16, 58), analysis of *BACE1*$^{-/-}$ MEF stably expressing wtBACE1 revealed predominant co-localization of wtBACE1 with γ-adaptin and transferrin receptor, which are markers of the TGN and endosomes, respectively (Fig. 2, *A* and *B*). Similar to wtBACE1, the BACE1-4C/A mutant also mainly localized to the TGN and endosomes.

The studies described above did not reveal any difference in TGN and endosome localization of wtBACE1 and BACE1-4C/A mutant suggesting that lack of *S*-palmitoylation did not affect the steady-state distribution of BACE1 in intracellular organelles. Next, we performed cell surface biotinylation studies to determine whether *S*-palmitoylation regulates the steady-state levels of BACE1 at the cell surface. In control N2a cells, following surface biotinylation ~5% of endogenous BACE1 bound to streptavidin beads, indicating that only a very small fraction of BACE1 is present at the cell surface at steady-state. Similar to endogenous BACE1, ~6% (WT, 6.24 ± 0.93, *versus* 4C/A, 6.82 ± 1.17) of stably overexpressed wtBACE1 and BACE1-4C/A was found to reside at the cell surface (Fig. 2*B*). Reprobing the same blots showed that >70% of CD147, a cell surface-localized type I transmembrane protein is isolated by this method in these experiments (Fig. 2*C*). Together, these results indicate that *S*-palmitoylation of BACE1 does not regulate intracellular or cell surface distribution of BACE1.

S-Palmitoylation Is Required for Association of BACE1 with Lipid Raft Membranes—*S*-Palmitoylation is an essential signal for lipid raft association of several soluble and integral membrane proteins (59). However, not all palmitoylated proteins are targeted to lipid rafts. Therefore, we were interested to determine the role of *S*-palmitoylation in lipid raft targeting of BACE1. Lipid rafts are biochemically defined as detergent-resistant membrane microdomains that resist extraction with detergents such as Triton X-100 and Lubrol at 4 °C (60). Although DRM isolated by biochemical fractionation differ in some characteristics from pre-existing lipid raft domains in live

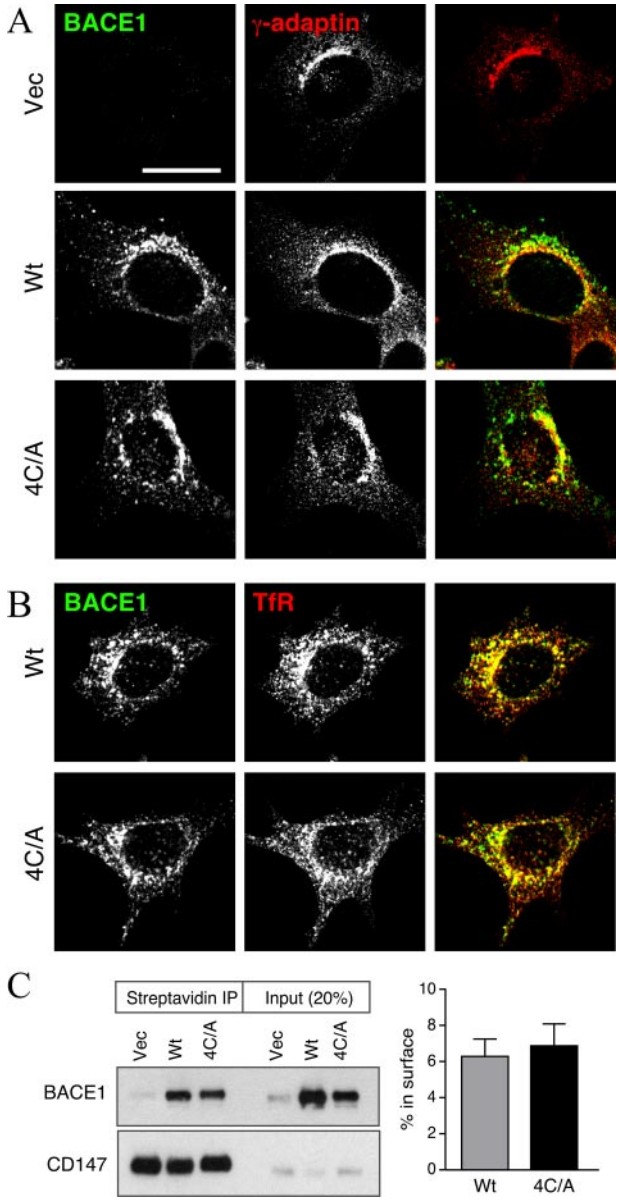

FIGURE 2. ***S*-Palmitoylation of BACE1 does not affect the subcellular distribution of BACE1.** *A* and *B*, confocal microscopy analysis of subcellular localization of BACE1. *BACE1*$^{-/-}$ MEF pools stably expressing wtBACE1 or BACE1-4C/A were co-stained with anti-BACE1 7523 antibody and the TGN marker γ-adaptin (*panel A*) or the recycling endosome marker transferrin receptor (*TfR*) (*panel B*). Note the absence of BACE1 staining in the vector-transfected *BACE1*$^{-/-}$ MEF. *Scale bar* represents 10 μm. *C*, analysis of cell surface BACE1. Subconfluent dishes of cells were surface biotinylated and the levels of cell surface BACE1 were examined by streptavidin capture of biotinylated proteins followed by immunoblotting. The blots were reprobed with antibodies against CD147, a cell surface protein. Values represent mean ± S.E. of three experiments.

cell membranes, DRM fractionation remains as the standard method to identify raft-targeting signals (36). In previous studies we characterized lipid raft association of γ-secretase as well as APP CTFs in cultured cells and mouse brain by fractionation of membranes solubilized in Lubrol WX (40, 41). We used the same strategy to assess DRM association of wtBACE1, BACE1-3C/A, and BACE1-4C/A. Membrane rafts from stably transduced *BACE1*$^{-/-}$ MEF pools were prepared on the basis of detergent insolubility and low buoyant density on sucrose density gradients, essentially as described (40). Fractions enriched

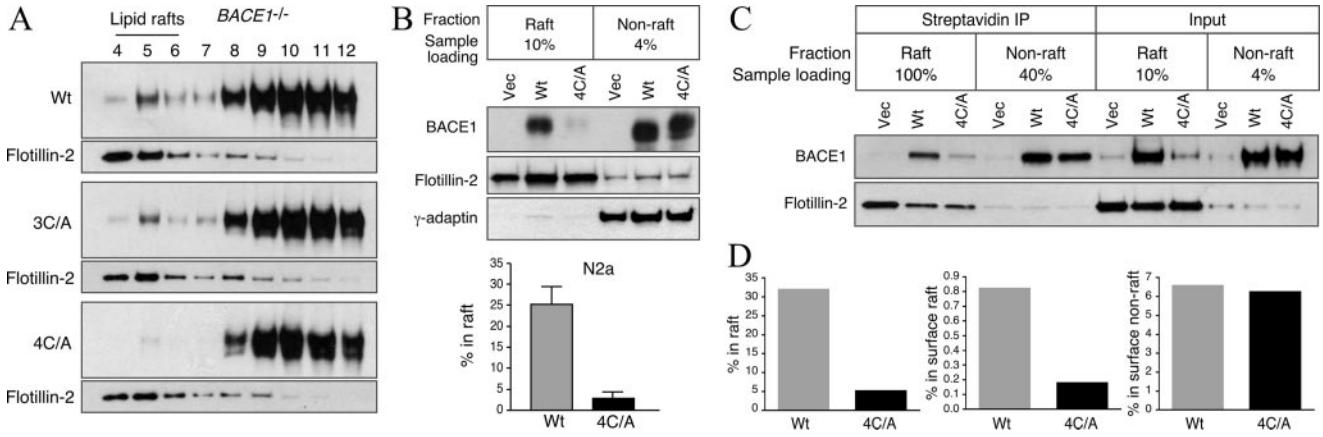

FIGURE 3. ***S*-Palmitoylation of BACE1 is required for DRM association.** *A* and *B*, sucrose density gradient fractionation of stable *BACE1*$^{-/-}$ MEF or N2a cells. Cells were solubilized in 0.5% Lubrol WX and subject to sucrose gradient fractionation. The gradients were harvested from the *top*, and the distribution of BACE1 was determined by Western blot analysis. Fractions containing lipid raft-associated proteins were identified by the presence of raft marker flotillin-2. Fractions 1–3 were excluded because there were no detectable signals for any of the proteins tested. In the case of N2a cells (*panel B*), raft (*4* and *5*) and non-raft (*8–12*) fractions were pooled and analyzed by Western blotting. The gels were loaded with 10% of pooled raft fractions and 4% of non-raft fractions. Signal intensities from Western blots were quantified as described under "Experimental Procedures" and plotted. Values represent mean ± S.E. of three experiments. *C*, raft association of BACE1 at the cell surface. Subconfluent dishes of N2a cells were surface biotinylated and then fractionated using sucrose gradient fractionation. Biotinylated proteins were isolated from pooled raft and non-raft fractions using streptavidin beads and analyzed by immunoblotting. Because of the differences in relative abundance, the gels were loaded with 100 (raft) or 40% (non-raft) of material bound to streptavidin-agarose, and 10 (raft) or 4% (non-raft) of input lysate. *D*, signal intensities of immunoblots were quantified and plotted.

in DRMs were identified by the enrichment of lipid raft marker, flotillin-2. In agreement with previous studies (37, 41), only a subset of wtBACE1 was recovered in gradient fractions enriched in flotillin-2 (Fig. 3*A*). We found a small decrease in the extent of DRM association of BACE1-3C/A mutant when compared with wtBACE1. On the other hand, the BACE1-4C/A palmitoylation-deficient mutant showed remarkable loss of DRM association (Fig. 3*A*). These results were confirmed by lipid raft fractionation of N2a neuroblastoma cells stably expressing wtBACE1 or BACE1-4C/A mutant (Fig. 3*B*). Quantification from three independent experiments showed that about 25% (25.18 ± 1.17) of wtBACE1 is found in fractions enriched in lipid rafts. Consistent with the results obtained from the *BACE1*$^{-/-}$ MEF described above, lack of *S*-palmitoylation resulted in a 10-fold reduction in raft association of BACE1-4C/A mutant (Fig. 3*B*).

Next, we examined raft and non-raft distribution of BACE1 localized at the plasma membrane. For these studies, we surface biotinylated stable N2a cells expressing wtBACE1 or BACE1-4C/A prior to lipid raft fractionation. Total cell surface proteins were isolated using streptavidin from pooled raft and non-raft fractions. Quantification of relative distribution of wtBACE1 showed that <1% wtBACE1 expressed in N2a cells is localized in cell surface DRMs, whereas about 6% of total wtBACE1 was found in detergent-soluble domains at the cell surface (Fig. 3, *C* and *D*). Analysis of cells expressing BACE1-4C/A revealed that lack of *S*-palmitoylation impaired cell surface raft association of mutant BACE1. However, as expected from surface biotinylation studies (Fig. 2*B*), the levels of WT and mutant BACE1 were similar in cell surface non-raft domains (Fig. 3, *C* and *D*). Together, these results indicate that *S*-palmitoylation at four Cys residues mediates lipid raft localization of BACE1 in both neuronal and non-neuronal cells.

S-Palmitoylation of BACE1 Is Not Required for APP Processing—The studies described above indicate that the lack of *S*-palmitoylation in BACE1 does not affect protein stability or subcellular localization but completely displaced BACE1 from lipid raft domains. Thus, the BACE1-4C/A mutant is ideal to ascertain the importance of lipid raft residence of BACE1 on APP processing without pharmacological manipulation of cellular cholesterol levels. To facilitate APP metabolism studies, we first retrovirally infected a stable N2a cell line overexpressing wtAPP (N2a 695.13) and generated a stable pool of cells expressing various levels of wtBACE1 or BACE1-4C/A. Quantifications from [^{35}S]Met/Cys labeling experiments indicate that the stable pools generated using pMX-IRES and pMX retroviral vectors overexpress BACE1 at 2- or 10-fold higher than endogenous BACE1 expression, respectively (Fig. 4*A*). Short pulse labeling with [^{35}S]Met/Cys showed that wtAPP expression is similar in the stable pools analyzed (data not shown). Continuous labeling for 3 h showed a marked reduction in the levels of mature APP in stable cells overexpressing wtBACE1, indicative of efficient processing by BACE1, as observed in previous studies (61). To confirm this notion, we examined the proteolytic products derived from BACE1 cleavage of APP, *i.e.* β-APP CTFs and sAPPβ. To determine the levels of β-APP CTFs we immunoprecipitated detergent lysates prepared from cells labeled for 3 h with [^{35}S]Met/Cys using APP C-terminal antibodies. Low level overexpression of wtBACE1 resulted in a small increase in the levels of APP β-CTFs +1 and +11 CTFs, relative to vector control cells (Fig. 4*B*). The increase in β-CTFs +1 and +11 CTFs was readily apparent in cells expressing wtBACE1 at high levels. Contrary to expectation, non-raft localized BACE1-4C/A also efficiently proteolyzed APP, and generated β-APP CTFs at levels comparable with that of wtBACE1. When the cells were treated with a γ-secretase inhibitor (Compound E), we observed a marked accumulation of APP CTFs as expected, but still found no quantitative differences in the levels of APP CTFs between cells expressing wtBACE1 or BACE1-4C/A (Fig. 4*B*). To confirm the above findings, we collected conditioned media and performed ELISA to quantify the levels of sAPPα and sAPPβ, derived from proc-

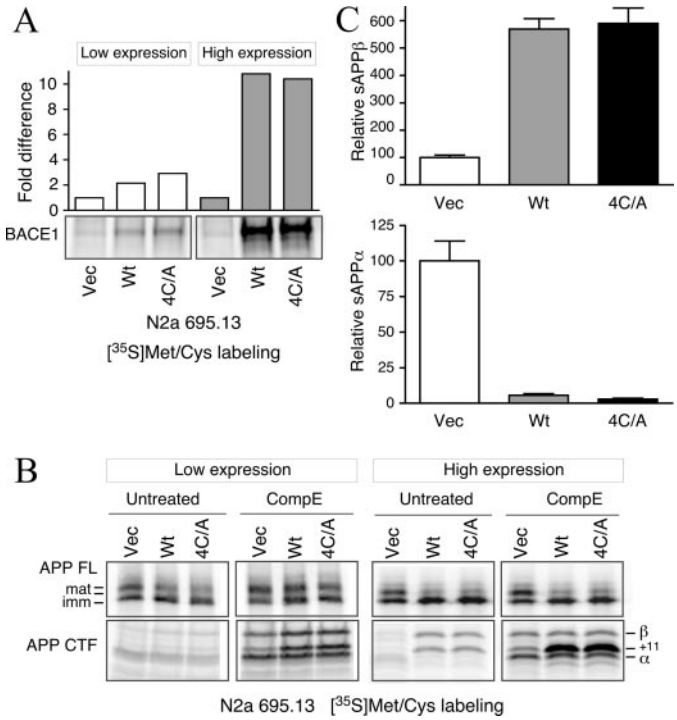

FIGURE 4. **Analysis of wtAPP metabolism.** *A*, quantitative analysis of BACE1 expression in low and high expressor pools. Stable pools of N2a 6951.3 cells were metabolically labeled with [^{35}S]Met/Cys for 3 h and BACE1 was immunoprecipitated from the cell lysate with anti-BACE1 antibody and analyzed by phosphorimaging. *B*, metabolic analysis of APP CTFs. Subconfluent dishes of N2a 6951.3 pools were treated with Me_2SO (vehicle) or Compound E (10 nM) for 16 h and metabolically labeled with [^{35}S]Met/Cys for 3 h in the presence of Me_2SO or Compound E. APP FL and APP CTFs were immunoprecipitated from equal amounts of total protein lysates with CTM1 antibody and analyzed by phosphorimaging. *C*, ELISA quantification of sAPPα and sAPPβ levels from medium conditioned by N2a 695.13 cells stably overexpressing wtBACE1 and 4C/A mutant. Values represent mean ± S.E. of three experiments.

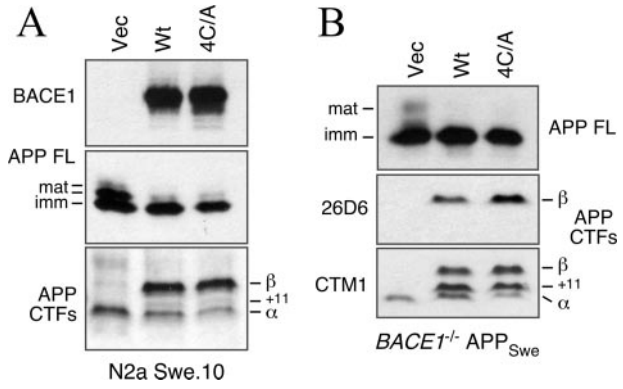

FIGURE 5. **Analysis of APP_{Swe} metabolism.** Subconfluent dishes of N2a Swe.10 (*A*) or *BACE1*$^{-/-}$ APP_{Swe} MEF (*B*) were lysed and equal amounts of total proteins were analyzed by Western blotting with antibodies against BACE1 and APP. APP FL and APP CTFs were detected by antibody CTM1 (raised against the C terminus of APP) and β-CTF were selectively detected using mAb 26D6 (epitope 1–12 of Aβ).

essing of APP by α- and β-secretase, respectively. Results showed that the levels of sAPPβ were markedly elevated with a concomitant decrease in the levels of sAPPα in cells overexpressing wtBACE1 as compared with vector cells. The levels of sAPPβ and sAPPα in the media of BACE1-4C/A cells were indistinguishable from that of wtBACE1 cells, providing direct evidence that *S*-palmitoylation does not contribute to BACE1 activity in cultured cells (Fig. 4*C*). Collectively, these results demonstrate that BACE1 processing of wtAPP in N2a cells was unaffected by lack of *S*-palmitoylation and the resulting non-raft localization of BACE1.

The FAD-linked "Swedish" APP variant (APP_{Swe}) differs considerably from wtAPP with respect to intracellular trafficking itinerary and subcellular site(s) of BACE1 processing (reviewed in Ref. 62). Therefore, we decided to analyze processing of APP_{Swe} by wtBACE1 and the BACE1-4C/A mutant. For these studies, we generated stable N2a cells co-expressing APP_{Swe} and wtBACE1 or BACE1-4C/A. Similar to what we observed in cells expressing wtAPP, stable overexpression of BACE1 resulted in marked reduction in the levels of mature APP_{Swe} and a concomitant increase in the levels of β-APP CTFs relative to APP_{Swe}/vector control cells (Fig. 5*A*). Overexpression of the BACE1-4C/A mutant also yielded similar levels of β-CTFs, further supporting our conclusion that BACE1-4C/A mutant is capable of efficiently processing APP. Finally, to formally rule out the contribution of endogenous wtBACE1, we generated *BACE1*$^{-/-}$ MEF co-expressing APP_{Swe} and wtBACE1 or BACE1-4C/A. As in N2a cells, we observed a marked reduction in mature APP and selective increase in β-CTFs upon low or high level expression of either wtBACE1 or BACE1-4C/A. β-APP CTFs originating at +1 were distinguished from that of +11 CTFs by selective detection of +1 CTFs using mAb antibody 26D6, which reacts with the N-terminal region of Aβ (Fig. 5*B*). These results indicate that BACE1 can efficiently cleave APP irrespective of post-translational modification by *S*-palmitoylation and localization in raft or non-raft microdomains.

Raft Association of APP CTFs—The results presented above indicate that the BACE1-4C/A mutant predominantly resides in non-raft membrane domains and is capable of processing APP when overexpressed in cultured cell lines. We reasoned that if APP processing by BACE1-4C/A mutant occurs in detergent-soluble membrane domains, we should be able to see quantitative differences in raft *versus* non-raft residence of APP CTFs in BACE1-4C/A cells as compared with wtBACE1 cells. To test this notion, we performed lipid raft fractionation of N2a 695.13 cells stably overexpressing wtBACE1 or BACE1-4C/A mutant. Cells were pretreated with 10 nM Compound E to block γ-secretase processing and cause accumulation of APP CTFs, which facilitates their detection. As expected, we found significant differences in raft *versus* non-raft distribution of APP CTFs between wtBACE1 and BACE1-4C/A cells (Fig. 6). In wtBACE1 cells, the majority of APP CTFs were found in DRM fractions. In the case of the BACE1-4C/A mutant, there is a considerable shift in the distribution of APP CTFs in the gradient toward the fractions containing detergent-soluble proteins. Quantifications revealed that in the case of wtBACE1, only 15% of APP CTFs was present in detergent-soluble non-raft fractions, whereas 44% of APP CTFs was recovered in non-raft fractions of BACE1-4C/A cells. Reprobing of the blots with raft-resident protein flotillin-2 and PS1 revealed no significant differences in the DRM distribution of these proteins between the cells (Fig. 5*A*). Thus, we observed a clear shift in the steady-state localization of APP CTFs to detergent-soluble mem-

branes in cells expressing BACE1-4C/A, indicative of BACE1-4C/A processing of APP in non-raft domains.

Analysis of Aβ Secretion in Cells Expressing S-Palmitoylation-deficient BACE1—In the experiments described above, we note that at steady-state the majority of APP CTFs in both wtBACE1 and BACE1-4C/A cells (85 and 56%, respectively) were found in lipid raft fractions, suggesting that APP CTFs may have intrinsic signals that facilitate raft recruitment, irrespective of the membrane microdomains where they are generated by BACE1 processing of APP FL. Because γ-secretase is also found in lipid rafts, one would predict little or no difference in the levels of Aβ generated in BACE1-4C/A cells, relative to wtBACE1 cells. To ascertain Aβ production we performed metabolic labeling with [^{35}S]Met/Cys in N2a cells coexpressing wtAPP and BACE1. By immunoprecipitation analysis of conditioned media we observed increased Aβ secretion by BACE1 overexpression, but found no quantitative differences between cells expressing wtBACE1 or BACE1-4C/A (Fig. 7*A*). We then quantified the levels of Aβ by ELISA using antibodies capable of detecting Aβ with heterogeneous N and C termini. These studies revealed that overexpression of BACE1 significantly increased the levels of secreted Aβ and that cells overexpressing wtBACE1 and BACE1-4C/A secreted very similar levels of Aβ species (Fig. 7, *B–D*). These results are consistent with APP FL processing by BACE1 in raft or non-raft domains followed by efficient processing of APP CTFs by γ-secretase.

DISCUSSION

Underlying eukaryotic cellular organization and function are the elaborate mechanisms that compartmentalize multiple biological activities not only in distinct organelles but also in specialized membrane microdomains. Evidence from multiple lines of investigations suggests that cholesterol-rich membrane microdomains are involved in the proteolytic processing of APP by transmembrane proteases BACE1 and γ-secretase (reviewed in Refs. 63 and 64)). Whereas the majority of APP CTFs and γ-secretase subunits associate with DRM (41), only a subset of BACE1 and APP FL in cultured cells and brain are found in DRM (34, 41). Aβ production in lipid rafts despite the discordant DRM distribution of APP FL *versus* APP CTF and BACE1 *versus* γ-secretase can be explained by two possible scenarios: first, only the subset of raft-associated APP FL are processed by BACE1, thus generating APP CTFs within lipid raft microdomains, which are subsequently processed by γ-secretase; second, a small fraction of APP FL undergoes BACE1 cleavage regardless of raft or non-raft membrane microdomain localization, and the resulting APP CTFs undergo γ-secretase cleavage within raft domains (34, 64). To explore these possibilities, we first characterized BACE1 *S*-palmitoylation at four Cys residues and report that site-directed mutagenesis of these Cys residues is sufficient to prevent BACE1 targeting to lipid rafts without altering BACE1 stability, maturation, or subcellular localization. We then compared APP processing by wtBACE1 or *S*-palmitoylation-deficient BACE1-4C/A mutant expressed in *BACE1*$^{-/-}$ MEF and N2a neuroblastoma cells, and document that the BACE1-4C/A mutant is capable of processing APP FL in non-raft domains. Moreover, we show that APP CTFs generated by BACE1-4C/A cleavage in non-raft domains subsequently become associated with lipid rafts and are processed to Aβ. Together these results suggest that BACE1 is targeted to lipid rafts following *S*-palmitoylation. However, *S*-palmitoylation-dependent raft localization of BACE1 is not prerequisite for amyloidogenic processing of APP.

Cholesterol is present in both leaflets of cellular membranes and plays an important role in stabilizing liquid-ordered lipid raft microdomains enriched in sphingolipids and cholesterol. Consequently, depletion of cholesterol disrupts lipid raft integrity (65). Previous efforts in characterizing BACE1 cleavage of APP in lipid rafts primarily relied on cholesterol depletion as the strategy to perturb raft association of APP and BACE1. The sensitivity of β-CTF and Aβ production to cellular cholesterol

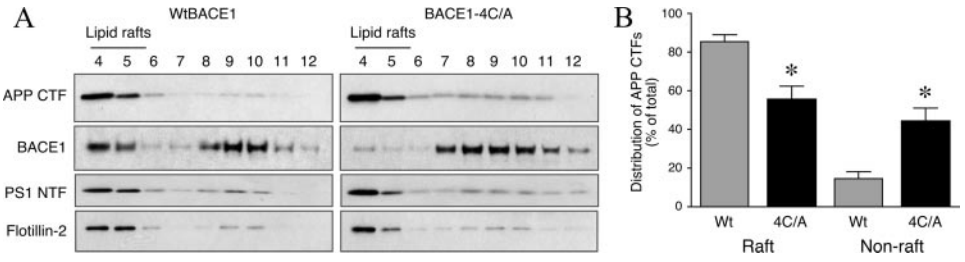

FIGURE 6. **DRM association of APP CTFs.** *A*, N2a 695.13 pools stably expressing wtBACE1 or BACE1-4C/A were treated with Compound E (10 nM) for 16 h and then lipid rafts were isolated by sucrose gradient fractionation. Raft and non-raft distribution of APP CTF was analyzed by Western blotting and the same blot was sequentially probed with antibodies against BACE1, PS1 N-terminal fragment, and flotillin-2. *B*, signal intensities of APP CTFs were quantified and plotted. Values represent mean ± S.E. of three experiments.

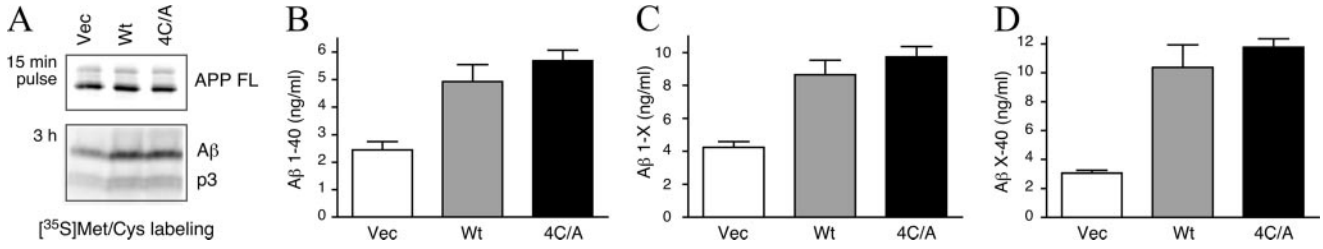

FIGURE 7. **Quantitative analysis of Aβ secretion.** *A*, N2a 695.13 pools stably expressing wtBACE1 or BACE1-4C/A were metabolically labeled with [^{35}S]Met/Cys for 15 min or 3 h. Lysates of cells labeled for 15 min were analyzed by immunoprecipitating with CTM1 to determine APP synthesis. Secreted Aβ was analyzed by immunoprecipitation of conditioned media from cells labeled for 3 h. *B–D*, ELISA quantification of conditioned media of stable N2a 695.13 pools was performed using mAb B113 capture/B436 detection (*Aβ1–40*); mAb B436 capture/4G8 detection (*Aβ1-x*); or mAb B113 capture/4G8 detection (*Aβx-40*). Values represent mean ± S.E. of three experiments.

depletion (with a combination of the lipophilic statin, lovastatin, and the cholesterol extracting agent methyl β-cyclodextrin), led to the conclusion that BACE1 processing of APP occurs within lipid rafts in cultured cells and neurons (32, 33). However, a recent report has challenged this view and suggested that membrane cholesterol levels can have a positive or negative effect on BACE1 processing of APP, depending on the extent of cholesterol depletion (34). Moderate loss of cholesterol in hippocampal neurons (<25% loss) facilitated colocalization of APP and BACE1 and increased Aβ production by promoting BACE1 cleavage of APP. In addition to these apparent discrepancies, proper interpretation of cholesterol depletion studies are confounded by the pleiotropic effects of cholesterol depletion on endocytosis, Golgi morphology, and vesicular trafficking, as well as perturbation in lateral diffusion of raft and non-raft proteins due to alterations in membrane fluidity and curvature (42, 43, 45–47). For example, as cholesterol-rich lipid microdomains are required for the biogenesis of secretory vesicles from the TGN (44), it is highly likely that secretory trafficking of APP, BACE1, and γ-secretase are all compromised in cells depleted of cholesterol. Moreover, the commonly used cholesterol-lowering agent lovastatin is known to have cholesterol-independent effects on APP trafficking and processing (66, 67). Thus it is difficult to draw unambiguous conclusions regarding BACE1 processing of APP in lipid raft domains solely based on cholesterol depletion studies.

In this study, we investigated the significance of BACE1 processing of APP in lipid rafts without altering cellular cholesterol levels. Protein acylation such as palmitoylation and myristoylation targets a variety of cytosolic and membrane proteins to lipid rafts due to the high affinity of acyl chains for the ordered lipid environment within raft domains (68). Because BACE1 was reported to be *S*-palmitoylated at three Cys residues within the cytoplasmic tail, we took advantage of this raft-targeting signal to study BACE1 processing of APP. In addition to the previously reported sites (Cys^{478}/Cys^{482}/Cys^{485}), we identified a fourth residue (Cys^{474}) within the transmembrane domain of BACE1 as a site that undergoes *S*-palmitoylation. Combined substitutions of the four Cys residues results in complete displacement of BACE1 from raft domains. It is interesting to note that the BACE1-3C/A mutant with only the single transmembrane *S*-palmitoylation site still could be labeled with [^{3}H]palmitic acid and continued to associate with lipid rafts (Figs. 1 and 2). Thus, the importance of tandem *S*-palmitoylation in BACE1 is currently unclear. In this regard, *S*-palmitoylation is a reversible modification mediated by a family of DHHC PATs and acylprotein thioesterases (reviewed in Ref. 54). In transfected COS cells at least five PATs (DHHC 3, 4, 7, 15, and 20) enhanced BACE1 *S*-palmitoylation (Fig. 1). Although our studies suggest that lack of *S*-palmitoylation did not affect subcellular localization of BACE1 in N2a neuroblastoma, COS, or MEF, the functional significance of this lipid modification in the context of neuronal trafficking is as yet unclear. It is important to note that the presence of *S*-palmitate on proteins such as α-amino-3-hydroxyl-5-methyl-4-isoxazole propionic acid receptor subunits, PSD-95, GAP-43, Huntingtin, SNAP-25, and synaptotagmin regulates their sorting and function in neuronal presynaptic and post-synaptic compartments (48, 54, 69, 70). In future studies we plan to investigate whether reversible *S*-palmitoylation, in combination with the unique subcellular distribution of substrate-specific PATs serves as a potential mechanism to fine tune BACE1 trafficking in neurons.

Flotation gradient analysis of DRM has provided important information over the years about the functional role of lipid rafts in numerous biological processes, and continues to be the most commonly used method to assess lipid raft association of proteins (reviewed in Ref. 36). However, there has been growing concern in the use of detergent resistance criteria to draw conclusions about association of proteins with nanoscale sized, short-lived, cholesterol-enriched membrane domains in intact cells (71). Whereas it is clear that raft marker proteins such as flotillins and caveolins readily partition into low buoyant density fractions, the main criticism of this biochemical method is the potential for detergents to create or cause mixing of membrane domains, thereby inducing the merger of proteins/lipids localized in spatially distinct membrane domains and organelles of intact cells. This appears not to be a problem when we use Lubrol WX for raft isolation. In earlier studies, we found no evidence of mixed raft patches containing both syntaxin 6 (raft-associated t-SNARE localized in TGN/TGN vesicles) and SNAP-23 (raft-associated t-SNARE localized at the plasma membrane) by magnetic immunoisolation, essentially ruling out a possible merger of detergent-resistant domains of different subcellular organelles during cell lysis or subsequent raft isolation procedure (40). Moreover, the marked difference in the phase separation of BACE1-3C/A and -4C/A mutants, which differ in just one palmitic acid modification, further supports the usefulness of the biochemical method to study raft association of BACE1 (Fig. 3). We also observed clear separation of wtBACE1 (~25% raft association) and BACE1-GPI (~90% raft association) using the DRM fractionation method (not shown). Still, unequivocal demonstration of clustered localization of BACE1 in cholesterol-rich microdomains will necessitate the direct imaging of intact cells at nanoscale resolution.

Antibody-induced copatching of proteins has been previously used to define raft association of APP and BACE1 at the plasma membrane (33, 39). When we used this method to assess copatching of PLAP and BACE-GPI, we made two unexpected observations. First, although the BACE1 and PLAP antibodies could successfully label the respective protein at the cell surface, we did not observe complete overlap between the patches formed by BACE1 and PLAP antibodies. Second, when analyzing % colocalization in randomly chosen cells expressing both proteins using Metamorph software, we noted that the extent of copatching observed between BACE1-GPI and PLAP strongly correlated with the average fluorescence intensity of each protein (*i.e.* their level of expression), indicating that the antibody co-patching approach might not be sensitive enough to detect subtle differences in lipid raft association of proteins when they are overexpressed (supplementary Fig. S1). Nevertheless, using stably transfected N2a cells with moderate overexpression of BACE1 we were able to visualize copatching of wtBACE1 with the lipid raft marker PLAP, and a small decrease in the extent of copatching between BACE1-4C/A and PLAP (supplementary Fig. S2). The major weakness in applying this

approach to study raft association of BACE1 is the paucity of BACE1 at the cell surface. We and others have estimated using cultured cells that only 5% of endogenous or overexpressed BACE1 is resident at the plasma membrane at steady-state (Fig. 2). Considering the complex mechanisms that regulate sorting of proteins and lipids at various stages of secretory and endocytic trafficking, sampling only a minor pool of BACE1 by imaging plasma membrane is unlikely to yield satisfactory estimation of the extent to which BACE1 associates with lipid rafts in cellular membranes.

Unlike what has been observed in many *S*-palmitoylated proteins such as chemokine receptor CCR5, human A1 adenosine receptor and Rous sarcoma virus transmembrane protein (reviewed in Ref. 54) lack of *S*-palmitoylation in BACE1 neither influenced protein stability nor subcellular localization. Nonetheless, WT and palmitoylation-deficient BACE1 mutants markedly differ in the extent of DRM association, enabling us to investigate the significance of BACE1 raft localization in APP processing. We performed detailed metabolic labeling studies to analyze APP β-CTF levels, and quantified sAPPα, sAPPβ, and Aβ levels by ELISA. These studies revealed that BACE1 processing of APP is indistinguishable in cells overexpressing wtBACE1 or BACE1-4C/A. To rule out potential protein overexpression artifacts, we confirmed these results using cells where BACE1 expression was only 2-fold higher than the endogenous levels. A measurable increase in the steady-state levels of APP CTFs in detergent-soluble fractions of BACE1-4C/A cells as compared with that of WT cells further strengthens our conclusion that palmitoylation-deficient BACE1 mutant efficiently cleaves APP in non-raft domains (Fig. 6). Although it is clear that *S*-palmitoylation and lipid raft localization of BACE1 is not obligatory for APP processing, they still might be important for the processing of other raft-localized BACE1 substrates such as neuregulin-1, lipoprotein receptor-related protein, or P-selectin-1 (72). It is also interesting to note that APP CTFs generated by BACE1-4C/A mutant are also recovered in DRM fractions. This finding indicates that APP CTFs may contain intrinsic signals that target them to cholesterol-rich membrane domains. Alternatively, ectodomain release following cleavage of APP FL by BACE1 or α-secretase relieves certain steric hindrance that underlies the paucity of APP FL in lipid rafts. Finally, it remains to be examined whether any of the multiple adaptors including Mint1, Mint2, Mint3, Dab1, and Fe65 that bind near the NPTY-motif in the cytosolic tail of APP facilitates raft association.

Acknowledgment—We thank Dr. Christian Haass for providing anti-BACE1 (7523) antibody.

REFERENCES

1. Vassar, R., Bennett, B. D., Babu-Khan, S., Kahn, S., Mendiaz, E. A., Denis, P., Teplow, D. B., Ross, S., Amarante, P., Loeloff, R., Luo, Y., Fisher, S., Fuller, J., Edenson, S., Lile, J., Jarosinski, M. A., Biere, A. L., Curran, E., Burgess, T., Louis, J. C., Collins, F., Treanor, J., Rogers, G., and Citron, M. (1999) *Science* **286,** 735–741
2. Sinha, S., Anderson, J. P., Barbour, R., Basi, G. S., Caccavello, R., Davis, D., Doan, M., Dovey, H. F., Frigon, N., Hong, J., Jacobson-Croak, K., Jewett, N., Keim, P., Knops, J., Lieberburg, I., Power, M., Tan, H., Tatsuno, G., Tung, J., Schenk, D., Seubert, P., Suomensaari, S. M., Wang, S., Walker, D., Zhao, J., McConlogue, L., and John, V. (1999) *Nature* **402,** 537–540
3. Yan, R., Bienkowski, M. J., Shuck, M. E., Miao, H., Tory, M. C., Pauley, A. M., Brashier, J. R., Stratman, N. C., Mathews, W. R., Buhl, A. E., Carter, D. B., Tomasselli, A. G., Parodi, L. A., Heinrikson, R. L., and Gurney, M. E. (1999) *Nature* **402,** 533–537
4. Cai, H., Wang, Y., McCarthy, D., Wen, H., Borchelt, D. R., Price, D. L., and Wong, P. C. (2001) *Nat. Neurosci.* **4,** 233–234
5. Cole, S. L., and Vassar, R. (2008) *J. Biol. Chem.* **283,** 29621–29625
6. Iwatsubo, T. (2004) *Curr. Opin. Neurobiol.* **14,** 379–383
7. Luo, Y., Bolon, B., Kahn, S., Bennett, B. D., Babu-Khan, S., Denis, P., Fan, W., Kha, H., Zhang, J., Gong, Y., Martin, L., Louis, J. C., Yan, Q., Richards, W. G., Citron, M., and Vassar, R. (2001) *Nat. Neurosci.* **4,** 231–232
8. Zhao, J., Fu, Y., Yasvoina, M., Shao, P., Hitt, B., O'Connor, T., Logan, S., Maus, E., Citron, M., Berry, R., Binder, L., and Vassar, R. (2007) *J. Neurosci.* **27,** 3639–3649
9. Li, Q., and Sudhof, T. C. (2004) *J. Biol. Chem.* **279,** 10542–10550
10. Lichtenthaler, S. F., Dominguez, D. I., Westmeyer, G. G., Reiss, K., Haass, C., Saftig, P., De Strooper, B., and Seed, B. (2003) *J. Biol. Chem.* **278,** 48713–48719
11. Kitazume, S., Tachida, Y., Oka, R., Shirotani, K., Saido, T. C., and Hashimoto, Y. (2001) *Proc. Natl. Acad. Sci. U. S. A.* **98,** 13554–13559
12. Koh, Y. H., von Arnim, C. A., Hyman, B. T., Tanzi, R. E., and Tesco, G. (2005) *J. Biol. Chem.* **280,** 32499–32504
13. Wong, H. K., Sakurai, T., Oyama, F., Kaneko, K., Wada, K., Miyazaki, H., Kurosawa, M., De Strooper, B., Saftig, P., and Nukina, N. (2005) *J. Biol. Chem.* **280,** 23009–23017
14. Hu, X., Hicks, C. W., He, W., Wong, P., Macklin, W. B., Trapp, B. D., and Yan, R. (2006) *Nat. Neurosci.* **9,** 1520–1525
15. Willem, M., Garratt, A. N., Novak, B., Citron, M., Kaufmann, S., Rittger, A., DeStrooper, B., Saftig, P., Birchmeier, C., and Haass, C. (2006) *Science* **314,** 664–666
16. Capell, A., Steiner, H., Willem, M., Kaiser, H., Meyer, C., Walter, J., Lammich, S., Multhaup, G., and Haass, C. (2000) *J. Biol. Chem.* **275,** 30849–30854
17. Creemers, J. W., Ines Dominguez, D., Plets, E., Serneels, L., Taylor, N. A., Multhaup, G., Craessaerts, K., Annaert, W., and De Strooper, B. (2001) *J. Biol. Chem.* **276,** 4211–4217
18. Walter, J., Fluhrer, R., Hartung, B., Willem, M., Kaether, C., Capell, A., Lammich, S., Multhaup, G., and Haass, C. (2001) *J. Biol. Chem.* **276,** 14634–14641
19. Benjannet, S., Elagoz, A., Wickham, L., Mamarbachi, M., Munzer, J. S., Basak, A., Lazure, C., Cromlish, J. A., Sisodia, S., Checler, F., Chretien, M., and Seidah, N. G. (2001) *J. Biol. Chem.* **276,** 10879–10887
20. Costantini, C., Ko, M. H., Jonas, M. C., and Puglielli, L. (2007) *Biochem. J.* **407,** 383–395
21. Huse, J. T., Pijak, D. S., Leslie, G. J., Lee, V. M., and Doms, R. W. (2000) *J. Biol. Chem.* **275,** 33729–33737
22. Koo, E. H., and Squazzo, S. L. (1994) *J. Biol. Chem.* **269,** 17386–17389
23. Haass, C., Lemere, C. A., Capell, A., Citron, M., Seubert, P., Schenk, D., Lannfelt, L., and Selkoe, D. J. (1995) *Nat. Med.* **1,** 1291–1296
24. Thinakaran, G., Teplow, D. B., Siman, R., Greenberg, B., and Sisodia, S. S. (1996) *J. Biol. Chem.* **271,** 9390–9397
25. Koo, E. H., Squazzo, S. L., Selkoe, D. J., and Koo, C. H. (1996) *J. Cell Sci.* **109,** 991–998
26. He, X., Zhu, G., Koelsch, G., Rodgers, K. K., Zhang, X. C., and Tang, J. (2003) *Biochemistry* **42,** 12174–12180
27. Shiba, T., Kametaka, S., Kawasaki, M., Shibata, M., Waguri, S., Uchiyama, Y., and Wakatsuki, S. (2004) *Traffic* **5,** 437–448
28. He, X., Li, F., Chang, W. P., and Tang, J. (2005) *J. Biol. Chem.* **280,** 11696–11703
29. Wahle, T., Prager, K., Raffler, N., Haass, C., Famulok, M., and Walter, J. (2005) *Mol. Cell. Neurosci.* **29,** 453–461
30. Wahle, T., Thal, D. R., Sastre, M., Rentmeister, A., Bogdanovic, N., Famulok, M., Heneka, M. T., and Walter, J. (2006) *J. Neurosci.* **26,** 12838–12846
31. Tesco, G., Koh, Y. H., Kang, E. L., Cameron, A. N., Das, S., Sena-Esteves, M., Hiltunen, M., Yang, S. H., Zhong, Z., Shen, Y., Simpkins, J. W., and Tanzi, R. E. (2007) *Neuron* **54,** 721–737

32. Simons, M., Keller, P., De Strooper, B., Beyreuther, K., Dotti, C. G., and Simons, K. (1998) *Proc. Natl. Acad. Sci. U. S. A.* **95,** 6460–6464
33. Ehehalt, R., Keller, P., Haass, C., Thiele, C., and Simons, K. (2003) *J. Cell Biol.* **160,** 113–123
34. Abad-Rodriguez, J., Ledesma, M. D., Craessaerts, K., Perga, S., Medina, M., Delacourte, A., Dingwall, C., De Strooper, B., and Dotti, C. G. (2004) *J. Cell Biol.* **167,** 953–960
35. Simons, K., and Toomre, D. (2000) *Nat. Rev. Mol. Cell. Biol.* **1,** 31–39
36. Brown, D. A. (2006) *Physiol.* (*Bethesda*) **21,** 430–439
37. Riddell, D. R., Christie, G., Hussain, I., and Dingwall, C. (2001) *Curr. Biol.* **11,** 1288–1293
38. Cordy, J. M., Hussain, I., Dingwall, C., Hooper, N. M., and Turner, A. J. (2003) *Proc. Natl. Acad. Sci. U. S. A.* **100,** 11735–11740
39. Sakurai, T., Kaneko, K., Okuno, M., Wada, K., Kashiyama, T., Shimizu, H., Akagi, T., Hashikawa, T., and Nukina, N. (2008) *J. Cell Biol.* **183,** 339–352
40. Vetrivel, K. S., Cheng, H., Lin, W., Sakurai, T., Li, T., Nukina, N., Wong, P. C., Xu, H., and Thinakaran, G. (2004) *J. Biol. Chem.* **279,** 44945–44954
41. Vetrivel, K. S., Cheng, H., Kim, S. H., Chen, Y., Barnes, N. Y., Parent, A. T., Sisodia, S. S., and Thinakaran, G. (2005) *J. Biol. Chem.* **280,** 25892–25900
42. Rodal, S. K., Skretting, G., Garred, O., Vilhardt, F., van Deurs, B., and Sandvig, K. (1999) *Mol. Biol. Cell* **10,** 961–974
43. Hansen, G. H., Niels-Christiansen, L. L., Thorsen, E., Immerdal, L., and Danielsen, E. M. (2000) *J. Biol. Chem.* **275,** 5136–5142
44. Wang, Y., Thiele, C., and Huttner, W. B. (2000) *Traffic* **1,** 952–962
45. Kirsch, C., Eckert, G. P., and Mueller, W. E. (2003) *Biochem. Pharmacol.* **65,** 843–856
46. Hao, M., Mukherjee, S., Sun, Y., and Maxfield, F. R. (2004) *J. Biol. Chem.* **279,** 14171–14178
47. Shvartsman, D. E., Gutman, O., Tietz, A., and Henis, Y. I. (2006) *Traffic* **7,** 917–926
48. Fukata, M., Fukata, Y., Adesnik, H., Nicoll, R. A., and Bredt, D. S. (2004) *Neuron* **44,** 987–996
49. Li, T., Ma, G., Cai, H., Price, D. L., and Wong, P. C. (2003) *J. Neurosci.* **23,** 3272–3277
50. Onishi, M., Kinoshita, S., Morikawa, Y., Shibuya, A., Phillips, J., Lanier, L. L., Gorman, D. M., Nolan, G. P., Miyajima, A., and Kitamura, T. (1996) *Exp. Hematol.* **24,** 324–329
51. Thinakaran, G., Regard, J. B., Bouton, C. M., Harris, C. L., Price, D. L., Borchelt, D. R., and Sisodia, S. S. (1998) *Neurobiol. Dis.* **4,** 438–453
52. Lamb, B. A., Bardel, K. A., Kulnane, L. S., Anderson, J. J., Holtz, G., Wagner, S. L., Sisodia, S. S., and Hoeger, E. J. (1999) *Nat. Neurosci.* **2,** 695–697
53. Vetrivel, K. S., Gong, P., Bowen, J. W., Cheng, H., Chen, Y., Carter, M., Nguyen, P. D., Placanica, L., Wieland, F. T., Li, Y. M., Kounnas, M. Z., and Thinakaran, G. (2007) *Mol. Neurodegener.* **2,** 4
54. Linder, M. E., and Deschenes, R. J. (2007) *Nat. Rev. Mol. Cell. Biol.* **8,** 74–84
55. Cheng, H., Vetrivel, K. S., Drisdel, R. C., Meckler, X., Gong, P., Leem, J. Y., Li, T., Carter, M., Chen, Y., Nguyen, P., Iwatsubo, T., Tomita, T., Wong, P. C., Green, W. N., Kounnas, M. Z., and Thinakaran, G. (2009) *J. Biol. Chem.* **284,** 1373–1384
56. McCormick, P. J., Dumaresq-Doiron, K., Pluviose, A. S., Pichette, V., Tosato, G., and Lefrancois, S. (2008) *Traffic* **9,** 1984–1997
57. Jonas, M. C., Costantini, C., and Puglielli, L. (2008) *EMBO Rep.* **9,** 916–922
58. Yan, R., Han, P., Miao, H., Greengard, P., and Xu, H. (2001) *J. Biol. Chem.* **276,** 36788–36796
59. Smotrys, J. E., and Linder, M. E. (2004) *Annu. Rev. Biochem.* **73,** 559–587
60. Brown, D. A., and London, E. (1998) *Annu. Rev. Cell Dev. Biol.* **14,** 111–136
61. Lee, E. B., Zhang, B., Liu, K., Greenbaum, E. A., Doms, R. W., Trojanowski, J. Q., and Lee, V. M. (2005) *J. Cell Biol.* **168,** 291–302
62. Vetrivel, K. S., and Thinakaran, G. (2006) *Neurology* **66,** S69–S73
63. Cordy, J. M., Hooper, N. M., and Turner, A. J. (2006) *Mol. Membr. Biol.* **23,** 111–122
64. Cheng, H., Vetrivel, K. S., Gong, P., Meckler, X., Parent, A., and Thinakaran, G. (2007) *Nat. Clin. Pract. Neurol.* **3,** 374–382
65. Harder, T., and Simons, K. (1997) *Curr. Opin. Cell Biol.* **9,** 534–542
66. Xiu, J., Nordberg, A., Shan, K. R., Yu, W. F., Olsson, J. M., Nordman, T., Mousavi, M., and Guan, Z. Z. (2005) *J. Neurosci. Res.* **82,** 531–541
67. Won, J. S., Im, Y. B., Khan, M., Contreras, M., Singh, A. K., and Singh, I. (2008) *J. Neurochem.* **105,** 1536–1549
68. Melkonian, K. A., Ostermeyer, A. G., Chen, J. Z., Roth, M. G., and Brown, D. A. (1999) *J. Biol. Chem.* **274,** 3910–3917
69. Hayashi, T., Saito, A., Okuno, S., Ferrand-Drake, M., Dodd, R. L., and Chan, P. H. (2005) *J. Cereb. Blood Flow Metab.* **25,** 41–53
70. Huang, K., and El-Husseini, A. (2005) *Curr. Opin. Neurobiol.* **15,** 527–535
71. Munro, S. (2003) *Cell* **115,** 377–388
72. Abbal, C., Lambelet, M., Bertaggia, D., Gerbex, C., Martinez, M., Arcaro, A., Schapira, M., and Spertini, O. (2006) *Blood* **108,** 3352–3359